

HIGH SNR PERFORMANCE ANALYSIS OF A BLIND FREQUENCY OFFSET ESTIMATOR FOR CROSS QAM COMMUNICATION

Stefania Colonnese, Gianpiero Panci, Stefano Rinauro and Gaetano Scarano

Dip. INFOCOM, "Sapienza" Universita' di Roma
via Eudossiana 18 00184 Roma, Italy
(colonnese, gpanci, rinauro, scarano)@infocom.uniroma1.it

ABSTRACT

In this paper we present theoretical performance analysis for a blind frequency offset estimator for cross Quadrature Amplitude Modulated constellations. The estimator is based on applying a tentative frequency offset compensation by means of a nonlinear transformation of the received signal samples and on estimating an accumulation function in different angular windows. For perfect frequency offset compensation, the measurements are suitably clustered and their accumulation, named "Constellation Phase Signature" (CPS), is a peaked function of the window orientation. Hence, the frequency offset estimator is selected by maximization of the peakness of the accumulation function. The performance analysis is shown to match the numerical simulations for medium to high values of SNR.

Index Terms— Frequency estimation, Quadrature amplitude modulation.

1. INTRODUCTION

In general Quadrature Amplitude Modulated (QAM) transmission, preliminary trained or blind carrier phase and frequency offset estimation needs to be performed at the output of the receiver. Although many standard communication systems adopt trained transmission, great bandwidth savings are achieved using blind estimators. Recently, in [1], the authors have introduced a nonlinear least-squares (NLS) estimator for joint carrier phase and frequency offset estimation, that minimizes the asymptotic (large sample) error variance. The NLS estimator, which is constellation dependent, requires gain/SNR knowledge and exhibits a performance degradation on cross constellations.

In [2] a novel blind frequency offset estimator for cross QAM constellations has been introduced extending the phase offset estimator presented in [3]. This estimator is based on the observation that, when the frequency offset is perfectly removed by preliminary compensation, a suitable nonlinear transformation of the received signal samples exhibits a particular phase distribution, named Constellation Phase Signature (CPS). In ideal, noise-free QAM signalling, the CPS is constituted by a discrete number of pulses whose locations depend on the signal constellation, and retains a significant peakness also in presence of channel noise. Hence, the frequency offset can be estimated by searching the frequency

compensation that maximizes the peakness of the CPS estimated on the compensated data. The resulting blind frequency estimator does not need neither gain/SNR nor constellation knowledge and performs well on cross constellations for medium to high values of SNR. Here we present analytical performance evaluation for the CPS estimator presented in [2].

This paper is organized as follows. In Sect.2 we introduce the model of the received signal, while in Sect.3 we recall the frequency estimator [2]. In Sect. 4 we present the performance analysis for the CPS estimator. Sect.5 shows results of both theoretical performance analysis and numerical simulations; for comparison sake, results of selected state-of-the-art estimators [1] are also reported.

2. DISCRETE-TIME SIGNAL MODEL

Let us consider a QAM communication system, and let $S[n]$ be the n -th transmitted symbol drawn from a power normalized M -ary constellation $\mathcal{A} = \{S_0, \dots, S_{M-1}\}$. At the receiver side, after front-end signal processing, a complex low-pass version of the received signal is available for sampling. Let us denote as $X[n]$ the samples of the received signal extracted at symbol rate. We will assume the following analytical model of the signal samples $X[n]$:

$$X[n] = G_C e^{j\theta + j2\pi f_e n} S[n] + W[n] \quad (1)$$

where G_C is the unknown overall gain, θ and f_e are the unknown phase and frequency offset, and $W[n]$ is a realization of circularly complex Gaussian stationary noise process, statistically independent of $X[n]$. The signal-to-noise ratio (SNR) is defined as $\text{SNR} \stackrel{\text{def}}{=} G_C^2 / \sigma_w^2$, being $\sigma_w^2 \stackrel{\text{def}}{=} \text{E} \{|W[n]|^2\}$ the noise variance.

We address the estimation of the carrier frequency offset f_e given a sample of N consecutive observations $X[n]$, $n = 0, \dots, N-1$. Due to the quadrant constellation¹ symmetry, without loss of generality, the frequency offset is limited to $|f_e| < 1/8$.

¹The quadrant constellation symmetry causes a $\pi/2$ ambiguity on the phase of the signal samples, which cannot be recovered in absence of side information.

3. CPS BASED FREQUENCY OFFSET ESTIMATION

Let us consider the following nonlinear function [1, 3, 2] of the received signal samples $X[n]$ under a frequency compensation of f_0 :

$$Y^{(f_0)}[n] = |X[n]|^P \cdot e^{j4 \cdot \arg\{X[n]\}} e^{-j2\pi 4 f_0 n} \quad (2)$$

Let us define the polar representation $Y^{(f_0)}[n] = r_n e^{j\varphi_n}$. In the noise free case, and for equiprobable constellation symbols, the pdf of the random variable $Y^{(f_0)}[n]$ is:

$$p_{R,\Phi}(r_n, \varphi_n; f_0) = \frac{1}{M} \sum_{m=0}^{M-1} \delta(r_n - (G_c |S_m|)^P) \cdot \delta(\varphi_n - 4\theta_n - 4 \arg S_m) \quad (3)$$

where $\theta_n = \theta + 2\pi(f_e - f_0)n$ is the time-variant phase-offset due to the residual frequency offset $f_e - f_0$.

For perfect frequency compensation $f_0 = f_e$, the noise-free pdf of the random variable $Y^{(f_0)}[n]$ becomes

$$p_{R,\Phi}(r, \varphi; f_e) = \frac{1}{M} \sum_{m=0}^{M-1} \delta(r - (G_c |S_m|)^P) \delta(\varphi - 4\theta - 4 \arg S_m) \quad (4)$$

From (3), (4), we see that for $f_0 \neq f_e$ the pdf of the random variable $Y^{(f_0)}[n]$ is cyclically shifted of $4\theta_n$ with respect to the variable φ , and $p_{R,\Phi}(r_n, \varphi_n; f_0) = p_{R,\Phi}(r, \varphi - 2\pi 4(f_e - f_0)n; f_e)$.

In presence of additive noise, the Dirac pulses appearing in (3) become wider pulses whose shape depends on the SNR and the noise pdf²; however, we can still observe the pdf cyclic shift by the time varying phase-offset θ_n due to the residual frequency offset $f_e - f_0$.

Now, we introduce the Magnitude Weighed Tomographic Projection³ (MWTP) of the probability density function (pdf) $p_{R,\Phi}(r, \varphi; f_e)$, namely:

$$g_{\Phi}^{(\mathcal{A}, f_e, P)}(\varphi) \stackrel{\text{def}}{=} \int_0^{+\infty} r \cdot p_{R,\Phi}(r, \varphi; \theta) dr \quad (5)$$

The MWTP $g_{\Phi}^{(\mathcal{A}, f_e, P)}(\varphi)$, like an ordinary pdf, can be estimated by subdividing the phase interval $[0, 2\pi]$ in K intervals and evaluating the normalized area of $g_{\Phi}^{(\mathcal{A}, f_e, P)}(\varphi)$ in the k -th phase interval. At this aim, let us define

$$f^{(\mathcal{A}, f_e, P)}(\psi) \stackrel{\text{def}}{=} \frac{K}{2\pi} \cdot \int_{\psi}^{\psi + 2\pi/K} g_{\Phi}^{(\mathcal{A}, f_e, P)}(\varphi) d\varphi \quad (6)$$

In the limit $K \rightarrow \infty$, $f^{(\mathcal{A}, f_e, P)}(\psi_k)$ tends to $g_{\Phi}^{(\mathcal{A}, f_e, P)}(\psi_k)$ where $\psi_k \stackrel{\text{def}}{=} 2\pi k/K$. The CPS $f^{(\mathcal{A}, f_e, P)}(\psi)$ depends on the constellation \mathcal{A} and is typically a function built up by a finite set of pulses whose locations and width depend on the

²For SNR values high enough the shape of the Dirac pulses reduces to the pdf of the imaginary component of the noise $W[n]$.

³See [3] for a closed form calculation of the MWTP of a generic QAM signal.

signal constellation and signal-to-noise power ratio, respectively, and it is exploited in [3] to develop a blind phase offset estimator for general QAM signals. For perfect compensation $f_e = f_0$ the CPS can be estimated as

$$\hat{f}^{(\mathcal{A}, f_e, P)}(\psi_k) \stackrel{\text{def}}{=} \frac{1}{N} \sum_{n=0}^{N-1} |Y^{(f_e)}[n]| d_K^k(Y^{(f_e)}[n])$$

$$d_K^k(Y) = \frac{K}{2\pi} \text{rect}_{2\pi/K}(\arg(Y) - 2\pi(k+1/2)/K)$$

$$k = 0, \dots, K-1$$

and, in the limit case of $K \rightarrow \infty$ [3], is an unbiased estimate of the MWTP $g_{\Phi}^{(\mathcal{A}, f_e, P)}(\psi_k)$, since:

$$\begin{aligned} \mathbb{E} \left\{ \hat{f}^{(\mathcal{A}, f_e, P)}(\psi_k) \right\} &= \frac{1}{N} \sum_{n=0}^{N-1} \mathbb{E} \left\{ |Y^{(f_e)}[n]| d_K^k(Y^{(f_e)}[n]) \right\} \\ &= \frac{1}{N} \sum_{n=0}^{N-1} \int_0^{+\infty} \int_0^{2\pi} r p_{R,\Phi}(r, \varphi; f_e) d_K^k(r e^{j\varphi}) dr d\varphi \\ &= f^{(\mathcal{A}, f_e, P)}(\psi_k), \quad k = 0, \dots, K-1, \end{aligned}$$

For $f_0 \neq f_e$ we have

$$\begin{aligned} \mathbb{E} \left\{ \hat{f}^{(\mathcal{A}, f_0, P)}(\psi_k) \right\} &= \frac{1}{N} \sum_{n=0}^{N-1} \mathbb{E} \left\{ |Y^{(f_0)}[n]| d_K^k(Y^{(f_0)}[n]) \right\} \\ &= \frac{1}{N} \sum_{n=0}^{N-1} \int_{2\pi k/K}^{2\pi(k+1)/K} \int_0^{+\infty} r p_{R,\Phi}(r, \varphi - 2\pi 4(f_e - f_0)n; f_e) dr d\varphi \\ &= \frac{1}{N} \sum_{n=0}^{N-1} f^{(\mathcal{A}, f_e, P)}(\psi_k - 2\pi 4(f_e - f_0)n) \end{aligned}$$

Hence, the expected value of the function $\hat{f}^{(\mathcal{A}, f_0, P)}(\psi_k)$ is a temporal average of N suitably shifted versions of the perfectly compensated CPS, *i.e.* $f^{(\mathcal{A}, f_e, P)}(\psi_k)$. Based on this observation, we design a frequency estimator the \hat{f}_{CPS} that best collapses the sample function $\hat{f}^{(\mathcal{A}, f_0, P)}(\psi_k)$ towards the perfectly compensated CPS, *i.e.* $f^{(\mathcal{A}, f_e, P)}(\psi_k)$, by maximizing the peakness $\hat{\mathcal{P}}(f_0)$ of the sample function $\hat{f}^{(\mathcal{A}, f_0, P)}(\psi_k)$. In formulas

$$\hat{f}_{CPS} = \arg \max_{f_0} \{ \hat{\mathcal{P}}(f_0) \}$$

$$\hat{\mathcal{P}}(f_0) \stackrel{\text{def}}{=} \frac{1}{K} \sum_{k=0}^{K-1} |\hat{f}^{(\mathcal{A}, f_0, P)}(\psi_k)|^4 \quad (7)$$

The estimator in (7) is completely blind, since it is constellation independent and doesn't need any gain/SNR control.

Following the approach in [4], the maximization of the peakness $\hat{\mathcal{P}}(f_0)$ of the sample function $\hat{f}^{(\mathcal{A}, f_0, P)}(\psi_k)$ can be performed in two steps, *i.e.* by first scanning the admissible range of f_0 , *i.e.* $[-1/8, 1/8]$, with step Δf_0 between candidate frequencies to evaluate an intermediate coarse estimate \hat{f}_c , and then by interpolating the estimate \hat{f}_c around

the maximum to obtain the fine estimate \hat{f}_{fine} . Here, we adopt a parabolic approximation for the peakness function around its maximum, yielding the following formula for the fine estimate \hat{f}_{fine} :

$$\hat{f}_{fine} = \hat{f}_c + \frac{1}{8} \Delta f_0 \frac{\hat{\mathcal{P}}(\hat{f}_c + \Delta f_0) - \hat{\mathcal{P}}(\hat{f}_c - \Delta f_0)}{\hat{\mathcal{P}}(\hat{f}_c + \Delta f_0) + \hat{\mathcal{P}}(\hat{f}_c - \Delta f_0) - 2\hat{\mathcal{P}}(\hat{f}_c)}$$

The parabolic approximation captures the local peakness variations and allows the estimator performance analysis to be carried out in closed form [4].

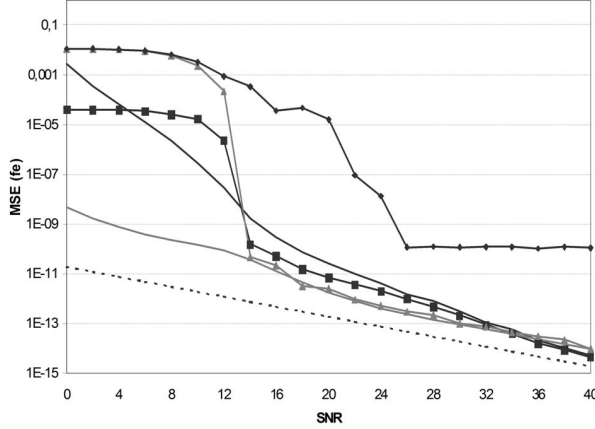


Fig. 1. MSE vs. SNR for 32-QAM constellation ($N = 2000, L = 512, P = 1$); CPS-based estimator (numerical: black square, theoretical: black solid line), NLS estimator in [1] (numerical: gray triangle, theoretical: gray solid line), 4th order estimator in [1] (diamond) and MCRB [5] (dashed line).

4. ANALYTICAL PERFORMANCE EVALUATION

In evaluating the accuracy of the estimator (3), we observe that two error components appear. The first component occurs when the coarse estimate \hat{f}_c is not correct, in the sense that it does not maximize the expected value of the peakness $\hat{\mathcal{P}}(k\Delta f)$ over the index k . The second error component is due to the sample peakness estimation error and to the misfit of the parabolic approximation around its maximum, and definitely limits the estimator accuracy. Numerical simulations show that, for a large range of SNR values, the coarse estimate is correct, and the first error component is zero. Hence, following the approach indicated in [4], the bias and the variance of \hat{f}_{fine} can be analytically evaluated as a function of the peakness mean, variance and covariances. Let us denote $E_{f_0} \stackrel{\text{def}}{=} \hat{\mathcal{P}}(f_0) - E\{\hat{\mathcal{P}}(f_0)\}$ and let us set the following positions $X = E\{\hat{\mathcal{P}}(f_c + \Delta f)\}$, $Y = E\{\hat{\mathcal{P}}(f_c - \Delta f)\}$, $Z = E\{\hat{\mathcal{P}}(f_c)\}$ and $c = X - Y$, $d = X - 2Z + Y$. Then, resorting to the following first-order approximation of (3):

$$\hat{f}_c - \hat{f}_{fine} \approx \frac{\Delta f}{8} \left(\frac{c}{d} + \frac{d-c}{d^2} E_{f_c + \Delta f} - \frac{d+c}{d^2} E_{f_c - \Delta f} - \frac{2c}{d^2} E_{f_c} \right)$$

we have obtained the following result:

$$\begin{aligned} \text{bias}(\hat{f}_{fine}) = & -\frac{\Delta f}{2} \frac{2}{d^3} \cdot \left[(Y - Z) \text{Var}(\hat{\mathcal{P}}(f_c + \Delta f)) \right. \\ & + (Z - X) \text{Var}(\hat{\mathcal{P}}(f_c - \Delta f)) - 2(X - Y) \text{Var}(\hat{\mathcal{P}}(f_c)) \\ & - (Y + 2Z - 3X) \text{Cov}(\hat{\mathcal{P}}(f_c - \Delta f), \hat{\mathcal{P}}(f_c)) \\ & + (Y + 2Z - 3X) \text{Cov}(\hat{\mathcal{P}}(f_c), \hat{\mathcal{P}}(f_c + \Delta f)) \\ & \left. - (X - Y) \text{Cov}(\hat{\mathcal{P}}(f_c + \Delta f), \hat{\mathcal{P}}(f_c - \Delta f)) \right] - b_{pm} \end{aligned}$$

where the term $b_{pm} = (f_e - f_c) + \Delta f \cdot 2 \cdot c/d$ accounts for the parabolic misfit [4]. As long as the variance of the estimator \hat{f}_{fine} is concerned, we have

$$\begin{aligned} \text{aVar}(\hat{f}_{fine}) & \stackrel{\text{def}}{=} \lim_{N \rightarrow \infty} N \cdot \text{Var}(\hat{f}_{fine}) \\ & = \frac{\Delta f^2}{64} \left[\left(\frac{d-c}{d^2} \right)^2 \text{Var}(\hat{\mathcal{P}}(f_c + \Delta f)) \right. \\ & + \left(\frac{d+c}{d^2} \right)^2 \text{Var}(\hat{\mathcal{P}}(f_c - \Delta f)) + \left(\frac{2c}{d^2} \right)^2 \text{Var}(\hat{\mathcal{P}}(f_c)) \\ & - \left(\frac{d^2 - c^2}{d^4} \right) \text{Cov}(\hat{\mathcal{P}}(f_c + \Delta f), \hat{\mathcal{P}}(f_c - \Delta f)) \\ & + \left(\frac{2dc + 2c^2}{d^4} \right) \text{Cov}(\hat{\mathcal{P}}(f_c), \hat{\mathcal{P}}(f_c - \Delta f)) \\ & \left. + \left(\frac{2dc - 2c^2}{d^4} \right) \text{Cov}(\hat{\mathcal{P}}(f_c + \Delta f), \hat{\mathcal{P}}(f_c)) \right] \end{aligned}$$

Now we derive the mean, variance and covariances of the sample peakness. Let us denote $f_P^{f_0}[k] = f^{(A, f_e, P)}(\psi_k)$ and let us define the zero mean random perturbation $\epsilon^{f_0}[k] = \hat{f}^{(A, f_0, P)}(\psi_k) - f_P^{f_0}[k]$. It follows that the peakness function can be written as:

$$\begin{aligned} \hat{\mathcal{P}}(f_0) & = \frac{1}{K} \sum_{k=0}^{K-1} \left(f_P^{f_0}[k] + \epsilon^{f_0}[k] \right)^4 \\ & \approx \frac{1}{K} \sum_{k=0}^{K-1} \left(f_P^{f_0}[k]^4 + 4f_P^{f_0}[k]^3 \epsilon^{f_0}[k] + 6f_P^{f_0}[k]^2 \epsilon^{f_0}[k]^2 \right) \end{aligned}$$

where we have discarded the terms $O(\epsilon^3)$. With this position, the moments of the peakness can be expressed as a function of the expected value $f_P^{f_0}[k]$ and of the moments of the variates $\epsilon^{f_0}[k]$. Let us now introduce the notations $m_{f_0}^{(r)}[k] \stackrel{\text{def}}{=} E\{(\epsilon^{f_0}[k])^r\}$, $m_{f_0}^{(r,s)}[k_1, k_2] \stackrel{\text{def}}{=} E\{(\epsilon^{f_0}[k_1])^r (\epsilon^{f_0}[k_2])^s\}$, $m_{f_0, f_1}^{(r,s)}[k_1, k_2] \stackrel{\text{def}}{=} E\{(\epsilon^{f_0}[k_1])^r (\epsilon^{f_1}[k_2])^s\}$.

The first and second order moments of the peakness are straightforwardly given by

$$E\{\hat{\mathcal{P}}(f_0)\} = \frac{1}{K} \sum_{k=0}^{K-1} \left(f_P^{f_0}[k]^4 + 6f_P^{f_0}[k]^2 m_{f_0}^{(2)}[k] \right)$$

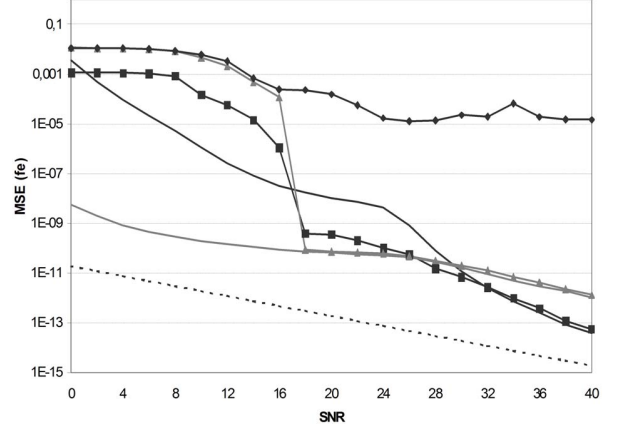
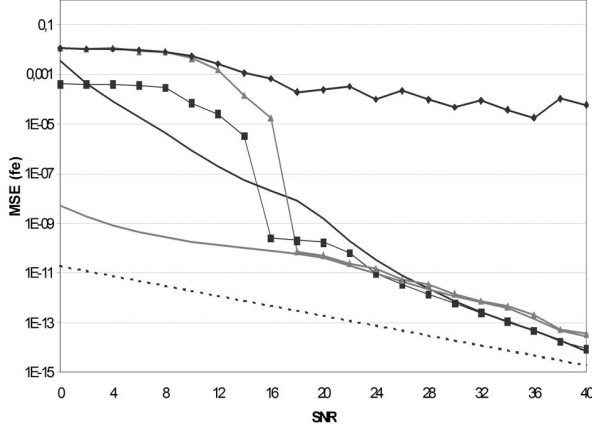


Fig. 2. MSE vs. SNR for 128-512 QAM constellation ($N = 2000, L = 512, P = 1$); CPS-based estimator (numerical: black square, theoretical: black solid line), NLS estimator in [1] (numerical: gray triangle, theoretical: gray solid line), 4th order estimator in [1] (diamond) and MCRB [5] (dashed line).

$$\begin{aligned}
 E\{\hat{\mathcal{P}}(f_0)^2\} &= \frac{1}{K^2} \sum_{k_1=0}^{K-1} \sum_{k_2=0}^{K-1} \\
 &\left(f_P^{f_0}[k_1]^4 f_P^{f_0}[k_2]^4 + 6f_P^{f_0}[k_1]^4 f_P^{f_0}[k_2]^2 m_{f_0}^{(2)}[k_2] \right. \\
 &+ 6f_P^{f_0}[k_2]^4 f_P^{f_0}[k_1]^2 m_{f_0}^{(2)}[k_1] + 16f_P^{f_0}[k_1]^3 f_P^{f_0}[k_2]^3 \\
 &\cdot m_{f_0}^{(1,1)}[k_1, k_2] + 36f_P^{f_0}[k_1]^2 f_P^{f_0}[k_2]^2 m_{f_0}^{(2,2)}[k_1, k_2] \left. \right) \\
 E\{\hat{\mathcal{P}}(f_0) \hat{\mathcal{P}}(f_1)\} &= \frac{1}{K^2} \sum_{k_1=0}^{K-1} \sum_{k_2=0}^{K-1} \left(f_P^{f_0}[k_1]^4 f_P^{f_1}[k_2]^4 \right. \\
 &+ 6f_P^{f_0}[k_1]^4 f_P^{f_1}[k_2]^2 m_{f_1}^{(2)}[k_2] + 6f_P^{f_1}[k_2]^4 f_P^{f_0}[k_1]^2 m_{f_0}^{(2)}[k_1] \\
 &+ 16f_P^{f_0}[k_1]^3 f_P^{f_1}[k_2]^3 m_{f_0, f_1}^{(1,1)}[k_1, k_2] \\
 &\left. + 36f_P^{f_0}[k_1]^2 f_P^{f_1}[k_2]^2 m_{f_0, f_1}^{(2,2)}[k_1, k_2] \right)
 \end{aligned}$$

where

$$\begin{aligned}
 m_{f_0}^{(2)}[k] &= \frac{1}{N^2} \sum_{n=0}^{N-1} \left(f_{2P}^{f_0}[k - \theta_n^{(f_0)}] - f_P^{f_0}[k - \theta_n^{(f_0)}] \right)^2 \\
 m_{f_0}^{(2)}[k, j] &= \frac{1}{N^2} \sum_{n=0}^{N-1} \left(f_{2P}^{f_0}[k - \theta_n^{(f_0)}] \delta_{kj} \right. \\
 &\quad \left. - f_P^{f_0}[k - \theta_n^{(f_0)}] f_P^{f_0}[j - \theta_n^{(f_0)}] \right) \\
 m_{f_0, f_1}^{(1,1)}[k, j] &= \frac{1}{N^2} \sum_{n=0}^{N-1} \left(f_{2P}^{f_0}[k - \theta_n^{(f_0)}] \delta_{k(j-L(f_0-f_1)n)} \right. \\
 &\quad \left. - f_P^{f_0}[k - \theta_n^{(f_0)}] f_P^{f_1}[j - \theta_n^{(f_1)}] \right)
 \end{aligned}$$

Finally, in the limit in which the sample error is asymptotically (large N) described by a normal distribution, we have:

$$\begin{aligned}
 m_{f_0}^{(2,2)}[k, j] &= m_{f_0}^{(2)}[k] m_{f_0}^{(2)}[j] + 2(m_{f_0}^{(1,1)}[k, j])^2 \\
 m_{f_0, f_1}^{(2,2)}[k, j] &= m_{f_0}^{(2)}[k] m_{f_1}^{(2)}[j] + 2(m_{f_0, f_1}^{(1,1)}[k, j])^2
 \end{aligned} \quad (8)$$

Let us remark that we used the approximation $f^{(A, f_0, P)}(\psi_k) \approx g_{\Phi}^{(A, f_0, P)}(\psi_k)$ for the numerical evaluation of the above reported first and second order moments of the peakness.

5. NUMERICAL EXPERIMENTS

Here, we present numerical results assessing the theoretical and experimental performance of the estimator introduced in Sect.3. Each experiment consists of 1000 Monte Carlo trials, each one with sample size $N = 2000$ and $\Delta f_0 = 1.4 \cdot 10^{-6}$; the value assumed for the frequency offset to be estimated is $f_e = 0.05 + \Delta f_0/4$. The experimental and theoretical Mean Square Error (MSE) of the frequency estimator \hat{f}_{CPS} introduced in Sect.3 versus SNR is shown in Figs.1 and 2 for 32-QAM, 128-QAM and 512-QAM. In Figs.1 - 2 we observe a good agreement between the analytical and the numerical performance for medium to high SNR. For comparison sake, we report also the results obtained using the optimal NLS estimator, requiring the knowledge of both the gain and the SNR, and the fourth order estimator in [1]. The CPS based estimator and the fourth order estimator in [1] are completely blind. The CPS based estimator outperforms the optimal estimator in [1] at high SNR while drastically outperforms the fourth order estimator in[1] at any SNR.

6. REFERENCES

- [1] Y. Wang, E. Serpedin, P. Ciblat, "Optimal blind nonlinear least-squares carrier phase and frequency offset estimation for general QAM modulations", *IEEE Transactions on Wireless Communications*, vol.2, Sept. 2003. Page(s):1040 - 1054.
- [2] S. Colonnese, G. Panci, S. Rinauro, G. Scarano, "Blind Carrier Frequency Offset Estimation for Cross QAM Constellation", ISWCS-2007, Trondheim, Norway, October 16-19 2007.
- [3] G. Panci, S. Colonnese, G. Scarano, "Asymptotically efficient phase recovery for QAM communication systems", ICASSP-2006, Toulouse, France, May 14-19, 2006.
- [4] G. Iacovitti, G. Scarano, "Discrete Time Techniques for Time Delay Estimation", *IEEE Trans. Sign. Proc.*, vol.2, February 1993.
- [5] A. N. D'Andrea, U. Mengali, R. Reggiani, "The modified Cramer Rao bound and Its applications at synchronization problems", *IEEE Transactions on Communications*, vol.42, Feb./Mar./Apr. 1994.